Comparative analysis of a large span gantry crane structure subjected to skewing force calculated using JUS and Eurocode 1 standards

Marko Todorović[1*], Goran Marković[1], Nebojša Zdravković[1], Mile Savković[1], Goran Pavlović[2]
[1]Faculty of mechanical and civil engineering in Kraljevo, University of Kragujevac, Kraljevo, Serbia
[2]Faculty of electronic engineering, University of Niš, Niš, Serbia

The way the skewing effect is being calculated differs between the JUS and Eurocode 1 standards. As a part of internal logistic systems many industries heavily rely on gantry cranes for their robustness and reliability which depend largely on the structure of the crane. Wire model of a truss structure of a gantry crane with approximately 60 m span used in timber industry was created and subjected to the loads in vertical plane and the skewing force in order to perform structural analysis using the finite element method for the skewing force calculated using both standards. The results of the conducted structural analysis were displayed in this paper.

Keywords: Large span gantry crane, finite element method, truss structure, structural analysis

1. INTRODUCTION

Every internal logistic system of an industrial facility or a warehouse as inseparable part of the larger scale logistic system is consisted of many different material handling devices. Cranes of all forms heavily participate in day-to-day operations as the only, or the most efficient way to transport the material from one place to another. Gantry cranes are especially important in timber industry where moving large and heavy logs is the central part of the operation.

Considering the high intensity loads gantry cranes are subjected to during their operation, their structure needs to be thoroughly analysed.

Many authors analysed causes and consequences of gantry crane breakdowns. In the [1] it was shown that a trivial design error such as use of passive rail clamps with half the required capacity can lead to derailment and failure of a gantry crane. Improper choice of the members of the gantry crane structure can lead to premature failure as it is shown in the paper [2] where improper thermic treatment of the crane wheels lead to derailment of the crane. The broken tooth phenomena in slewing bearing's large gear rings was studied in [3] as it has a great impact on the production efficiency of Chinese ports which causes huge economic losses. As gantry cranes are used in many different environments where people interact with the devices, the cranes have a part in the occupational accident risk analysis [4].

Since the failure of gantry cranes can cause great material damage and they have negative impact on the occupational safety of the workers, it is imperative to design the cranes that can withstand the loads they are being loaded with during their operation. In order to accomplish this, many methods and procedures for structural and dynamic analysis of the crane structures and components had been developed, where the numerical methods took the lead. Dynamics analysis of the cranes attracted a lot of interest from the researches. The authors of the [5] studied the dynamic behaviour of a nonlinear gantry crane system using the dynamic model that was derived using Lagrange equations. Transverse and longitudinal vibrations of a gantry crane system where the moving body was considered as a moving oscillator obtained using a numerical, combined finite element method and analytical method was studied in [6].

In structural analysis the effects of dynamic behaviour of the structure are usually taken into account by introducing the dynamic coefficients which are applied on the static loads [7]. These coefficients are usually built into standards that regulate loads the structure of the crane has to withstand, such as [8]–[10].

Numerical methods such as finite element methods were largely used for structural analysis singled out components of the cranes observing how common mechanical phenomena effect their structure. In the paper [11] such analysis was done on a main grinder of a single grinder portable gantry crane. Finite element analysis was also used in order to determine the effect of the main grinder cross section on the levels of generated stress [12]. In the paper [13] the strength analysis of the overhead traveling crane was conducted using the finite element methods with Abaqus, finite element analysis software.

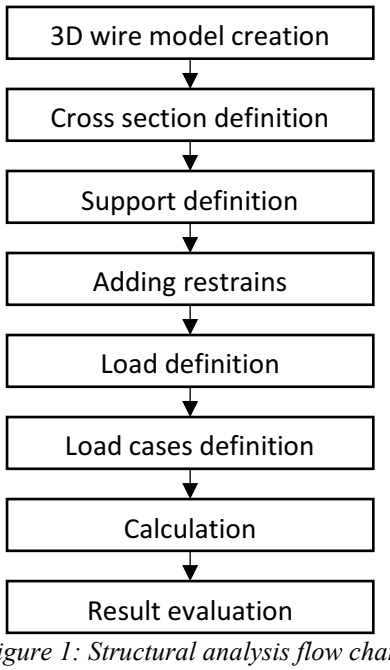

Figure 1: Structural analysis flow chart

*Corresponding author: Dositejeva 19, 36000 Kraljevo, Serbia, todorovic.m@mfkv.kg.ac.rs

However, there are not many papers focused on structural analysis of the whole gantry crane structure, which is the gap this paper is set to fill. The structural analysis will be completed using Autodesk Robot Structural Analysis software on a large span gantry crane structure. The structure of the paper follows the steps shown in Figure 1.

2. THE MODEL CREATION

The observed gantry crane, displayed in Figure 2, consists of two legs, one rigid and one elastic, connected with the main grinder with the span of 60.95 m. On each side there is an overhang. If the rigid leg is considered to be on the left side, and the elastic leg on the right side of the crane, the overhang on the left side is 15.9 m long, while the length of the overhang on the right side is 10.6 m. Total lifting capacity of the crane is set to be 50 kN. The lifting hight 7.6 m while the main grinder is on the 12.58 m distant from the ground plane.

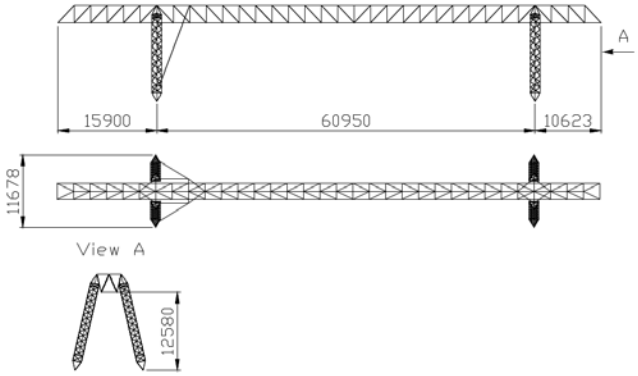

Figure 2: Large span gantry crane

The crane is used for moving logs in timber industrial facility. The hoist is equipped with grabbing device for lifting the logs. The weight of the grabbing device is 15 kN, while the weight of the hoist with the cabin for the operator combined equals 25 kN.

2.1. Three-dimensional wire model of the crane

The three-dimensional model of the crane was created from the available documentation and it is consisted of lines drawn in three-dimensional space where each line represents a member of the truss structure of the gantry crane. For creating the three-dimensional wire model, displayed in Figure 3, a CAD software was used, and the drawing was exported to .dxf format.

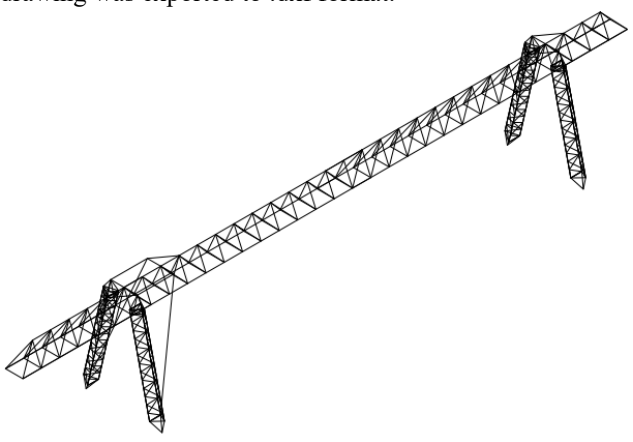

Figure 3: Isometric view of the three dimensional wire model of the gantry crane

2.2. Cross section definition

After the creation of the three-dimensional wire model of the gantry crane, and after it was exported to the .dxf format, as such it can be imported into the software for structural analysis and simulation using the finite element method, which can be seen in figure 4. In this software the lines that make the wire model are given physical properties: geometrical properties of the cross section as well as the properties of the material from which they are consisted.

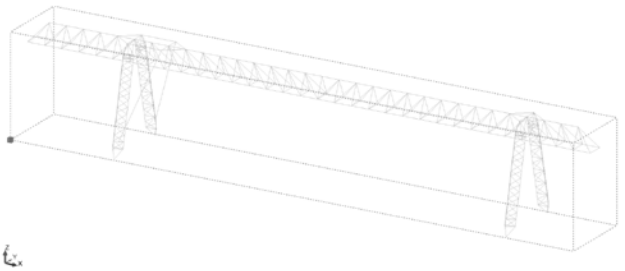

Figure 4: Three dimensional wire model imported into Autodesk Robot Structural Analysis

Each line of the wire model represents the one-dimensional finite element – the beam. In Figure 5 the model with assigned cross sections and materials is displayed.

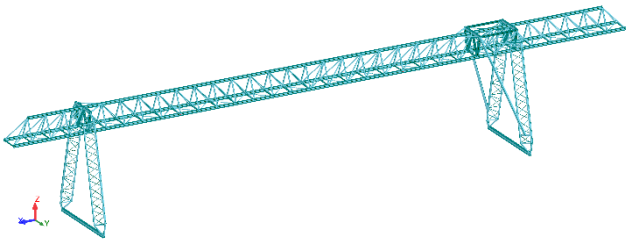

Figure 5: Three dimensional wire model with cross sections assigned to finite elements

Geometrical properties of the cross sections assigned to the members of the structure, surface areas and axial moments of inertia for all three local axes, are given in tables 1 and 2.

Table 1: List of used standard profiles and their surface areas

Profile	*AX [cm²]*	*AY [cm²]*	*AZ [cm²]*
2 CAE100x10	38.31	20	20
2 UPE360	155.8	74.8	86.4
2 UPN350	151.67	63.21	94.09
HE200A	53.83	38.68	13.28
IPN360	96.91	55.46	45.66
ROND50	19.63	16.57	16.57
ROND90	63.62	53.68	53.68
TREC100x50x5	13.88	6.17	6.17
TRON139x4	17.05	8.53	8.53
TRON168x4.5	23.16	11.58	11.58
TRON 323x5.6	56	28	28

Table 2: List of used standard profiles and their axial moments of inertia

Profile	*IX [cm⁴]*	*IY [cm⁴]*	*IZ [cm⁴]*
2 CAE100x10	12.67	353.4	6168.03
2 UPE360	24939.43	29650	11734.12
2 UPN350	111.9	25680	9379.22
HE200A	18.6	3692.15	1335.51
IPN360	118	19566	817.56
ROND50	61.36	30.68	30.68
ROND90	644.13	322.06	322.06
TREC100x50x5	134.6	169.9	55.06
TRON139x4	785.72	392.86	392.86
TRON168x4.5	1554.43	777.22	777.22
TRON 323x5.6	14188	7094.01	7094.01

All finite elements were assigned the same material property. Structural steel S355 was used for the whole structure. This material was modelled in the software using the data displayed in Table 3.

Table 3: Material properties

Material	E [MPa]	G [MPa]	ν	ρ [kN/m³]	Re [MPa]
S 355	210000	81000	0.3	77.01	355

…where E denotes the modulus of elasticity, G denotes the shear modulus, ν is Poisson's ratio, ρ is material density, and Re is yield strength.

2.3. Structure supports

Various load combinations that are defined by different standards require different ways of supporting the structure. However, for the most of the needed load combinations according to [9] and [14], the supports are defined as displayed in figure 6 and 7 where the two supports in nodes 1 and 260 are set to be fixed in all three directions, and the nodes 159 and 209 are fixed in the vertical (z) and traverse (x) direction while the movement in the y direction, direction in which the crane moves, is allowed.

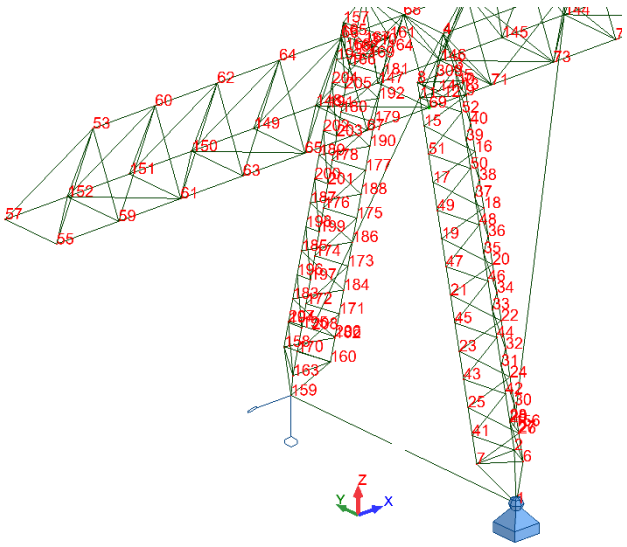

Figure 6: Supports in nodes 1 and 159

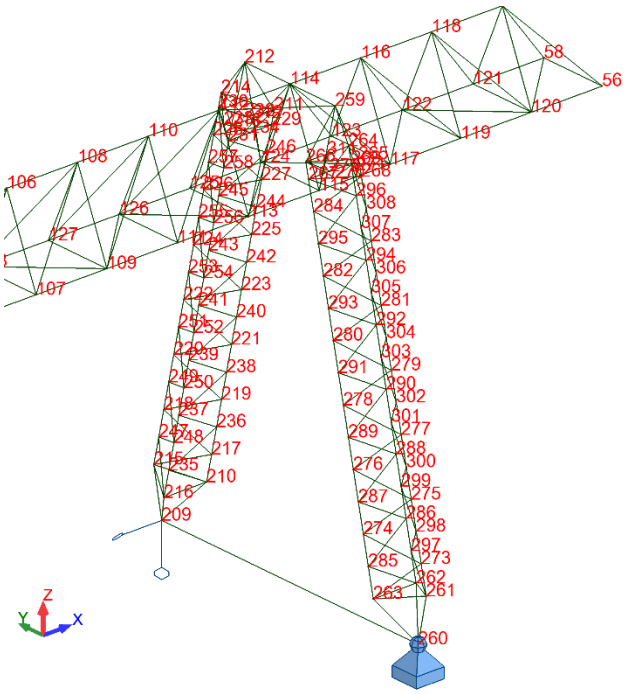

Figure 7: Supports in nodes 209 and 260

2.4. Releases

Based on the available documentation and photographs of the crane structure, it was concluded that the main grinder was connected to the crane legs with a pin in the global x direction which means that the momentum around the global x axis is not carried onto the crane legs. In the Figure 8 the releases in joints which form the described connection are shown.

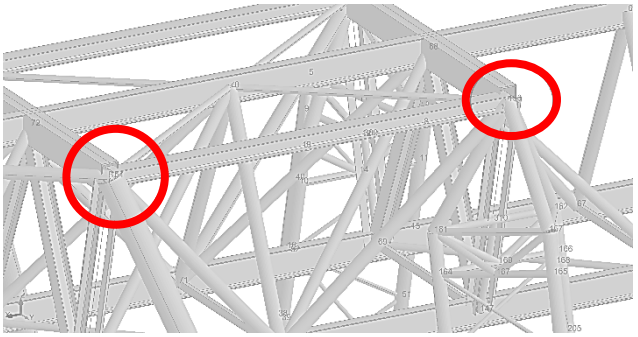

a) Releases for the riggid leg

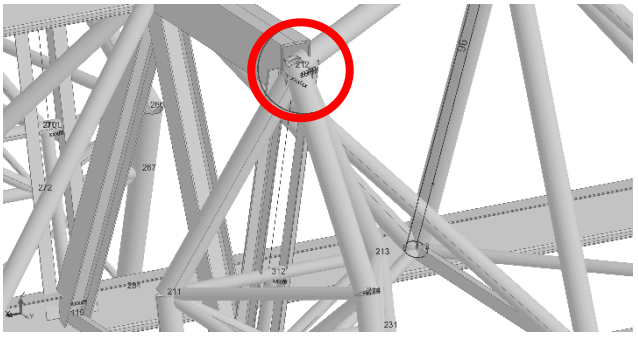

b) Releasess for the elastic leg

Figure 8: Releases in the connection between legs and the main grinder

The legs are also connected to the grinder via the pipe that is pinned on both sides, which is displayed in the Figure 9. Pinned connections assumes that moments around

any of the global axis do not get transferred with that connection. The connection between the beam that stiffens the rigid leg and the top of the lower part of the leg is in the form of a pin. This release is shown in the Figure 10.

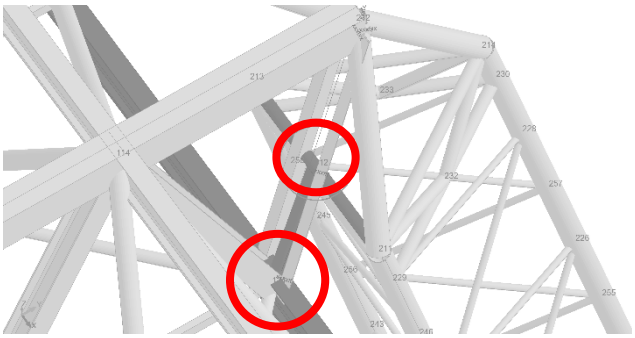

Figure 9: Releases for the bar pinned on both ends

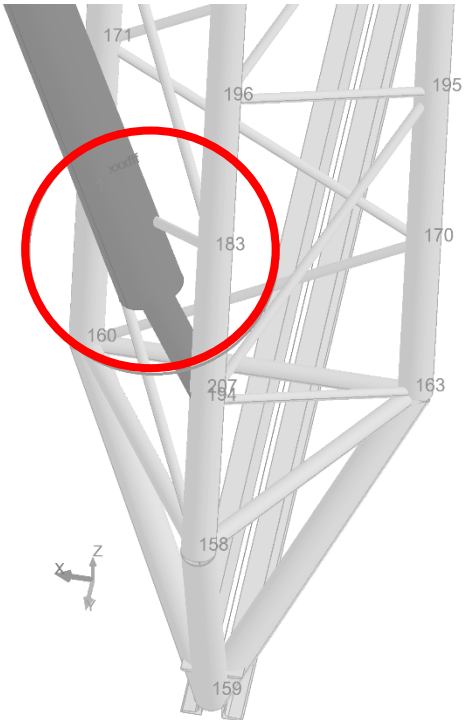

Figure 10: Releases between the crane leg and the stiffner

3. LOAD DEFINITION

The loads can be divided into two groups of loads, depending on the plane in which their vectors lay, to vertical and horizontal loads [9].

The vertical loads come from the weight of the crane structure, the weight of hoist, and the weight of the lifted load. Since the crane has a large span, the cabin for the operator is mounted to the hoist. It is considered that the resultant of the weight of the hoist and the cabin is located in the centre of the hoist, and that the weights of the hoist, cabin and lifted load is equally distributed on the wheels of the hoist, as it is show in the Figure 11, where R_1, R_2, R_3 and R_4 are the reactions, and the Q_t is the sum of the weight of the hoist Q_h, the cabin Q_c, the grabbing device Q_g and the lifted load Q_l:

$$Q_t = Q_h + Q_c + Q_g + Q_l \quad (1)$$

$$R_1 = R_2 = R_3 = R_4 = \frac{Q_t}{4} \quad (2)$$

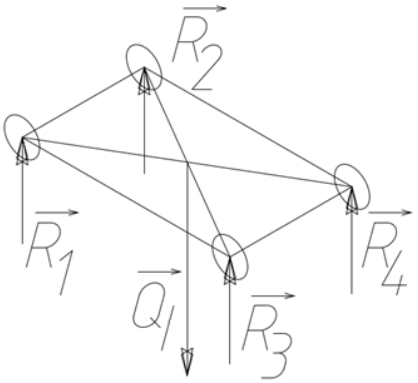

Figure 11: Reactions in the wheels of the loaded hoist

The values of the weights, as well as the intensities of the reactions on the wheels of the hoist are given in the table 4. When the hoist is empty, meaning it does not carry any useful load, as shown in the Figure 12, the values of the reactions on the hoist wheels are presented in Table 5.

Table 4: Table of weights and reactions

Denotation	Value [kN]	Description
Q_{cr}	530.02	Weight of the crane
Q_h	25	Weight of the hoist
Q_c		Weight of the cabin
Q_g	15	Weight of the grabbing device
Q_l	50	Weight of the load
R_1, R_2, R_3, R_4	22.5	Reactions

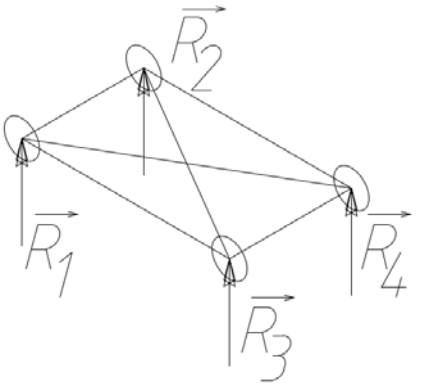

Figure 12: Reactions in the wheels of the empty hoist

Table 5: Table of weights and reactions in the wheels of the hoist

Denotation	Value [kN]	Description
Q_{cr}	530.02	Weight of the crane
Q_h	25	Weight of the hoist
Q_c		Weight of the cabin
Q_g	15	Weight of the grabbing device
Q_l	0	Weight of the load
R_1, R_2, R_3, R_4	10	Reactions

When it comes to the load in the horizontal plane, for the sake of comparison of the two standards, the focus of will be on the skewing forces. The skewing forces are defined differently in JUS and Eurocode 1 standards as the JUS standard defines the skewing load which acts on the structure of the crane above the elastic leg while the Eurocode 1 standard defines the skewing forces for the wheels of the crane.

In the Figure 13, the horizontal and vertical loads

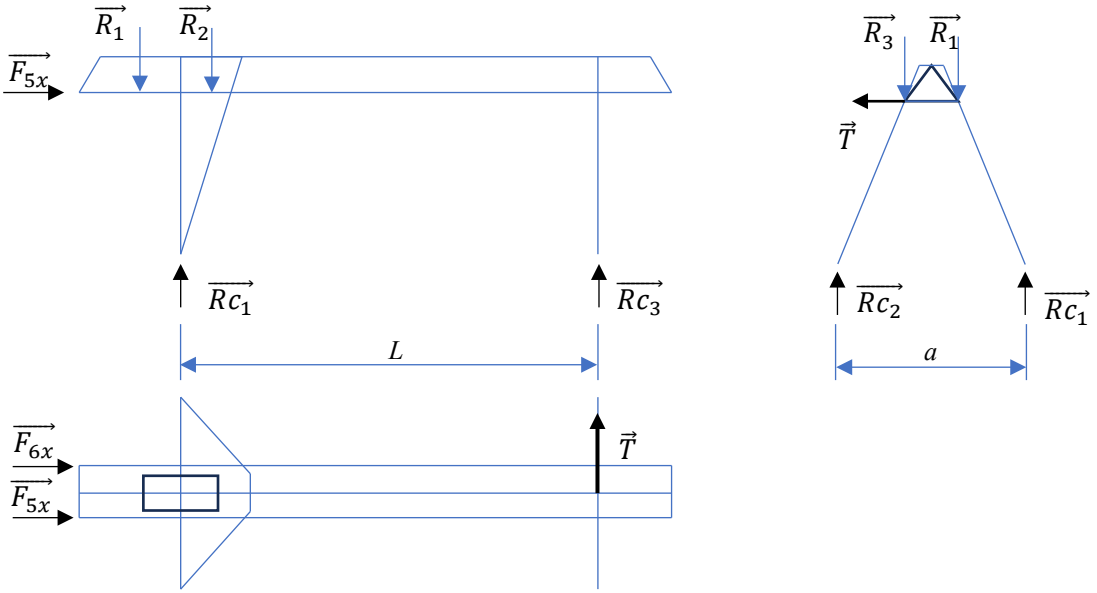

Figure 13: Crane with horizontal forces needed for calculating skewing load according to JUS standard

needed for calculating the intensity of the skewing force $\vec{T}$ are shown. According to the JUS standards [14], the intensity can be calculated using the following equation:

$$T = \frac{F_{H,max} \cdot a}{L} \quad (3)$$

$$F_{H,max} = \max(R_{C1}, R_{C2}, R_{C3}, R_{C4}) \cdot \lambda \quad (4)$$

For the case when the loaded hoist is located above the rigid leg, the values of the reactions of the crane wheels are given in the table 6. The parameter λ is the function of the ratio of traverse and longitudinal distance between the crane wheels, and in this case, according to [14] equals 0.1305. The intensity of the skewing force is given in the table 6.

Table 6: Reactions in crane wheels for the case when the loaded hoist is located above the rigid leg and the intensity of the skewing force

R_{C1} [kN]	R_{C2}[kN]	R_{C3}[kN]	R_{C4}[kN]	T [kN]
211.56	211.52	129.49	129.45	5.291

The forces F_{5x} and F_{6x} are forces that are taking into account the slipping of the wheels of the rigid leg [14], and they can be calculated as follows:

$$F_{5x} = 0{,}1 \cdot R_{C1}; F_{6x} = 0.1 \cdot R_{C2} \quad (5)$$

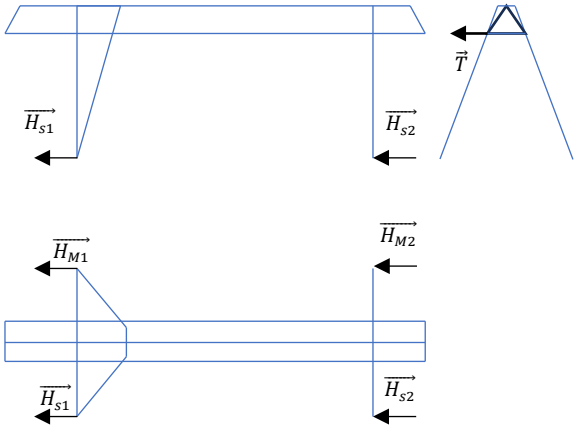

Figure 14: Skewing force displaced on the structure of the crane

The Eurocode 1 standard defines the skewing forces for each of the crane wheels individually. However, considering that the crane wheels in this case are modelled as supports for the structure within the software for finite element structural analysis, the forces in horizontal plane defined by the standard have to be displaced to the structure itself in order to be properly taken into account. As a step in this process, the forces from the individual wheels of the crane can be replaced with the appropriate forces for the group of the wheels H_{S1} and H_{S2}, as presented in the Figure 14. The momentum from displacing the forces can be replaced with the coupling of forces H_{M1} and H_{M2}. The intensity of the skewing force can finally be expressed as following:

$$T = \frac{a \cdot (HS - HM)}{2L} \quad (6)$$

$$HS = H_{S1} + H_{S2} \quad (7)$$

$$HM = H_{M1} + H_{M2} \quad (8)$$

The intensity of the skewing force T calculated using equations (6)-(8) for the specific case equals 4.922 kN.

The skewing force $\vec{T}$ is placed on the structure, as displayed in figure 13 and 14, above the elastic leg of the crane for both, JUS standard and Eurocode 1 cases.

After the forces are calculated, the loading cases are to be defined. The loads that are being taken into account for each load case with the proper dynamic coefficients are displayed in table 7. The loads are multiplied by coefficients and as such are used for the calculation. For this load case it is considered that the loaded hoist is located above the rigid leg as displayed in the Figure 13. The force of the wind is neglected, as well as the horizontal forces from the acceleration and deceleration of the crane.

Table 7: Load case definition

Load case: Skewing	
Load name	Coefficient value
Self-weight of the crane	1,1
Self-weight of the hoist	1,1
Self-weight of the load	1,1
Skewing load	1,0

4. RESULTS

After the model creation and after the calculation was finished the minimal and maximum stress distribution for both JUS and Eurocode 1 cases stayed similar, and it is displayed in figure 15.

The global maximum of the stress in both cases is in the member 353. One node of the member is the joint between the elastic leg of the crane and the main grinder, and the member itself is a part of the elastic leg. The load and stress distribution in the local coordinate system of the member 353 is displayed in the Figure 16 for the both observed cases. In the table 8 the values of the stresses were compared between the cases for the member 353. The same diagrams are given for the main grinder beam with the highest stress value in the Figure 17. The numerical values of the calculation results for the beam are displayed in the table 9.

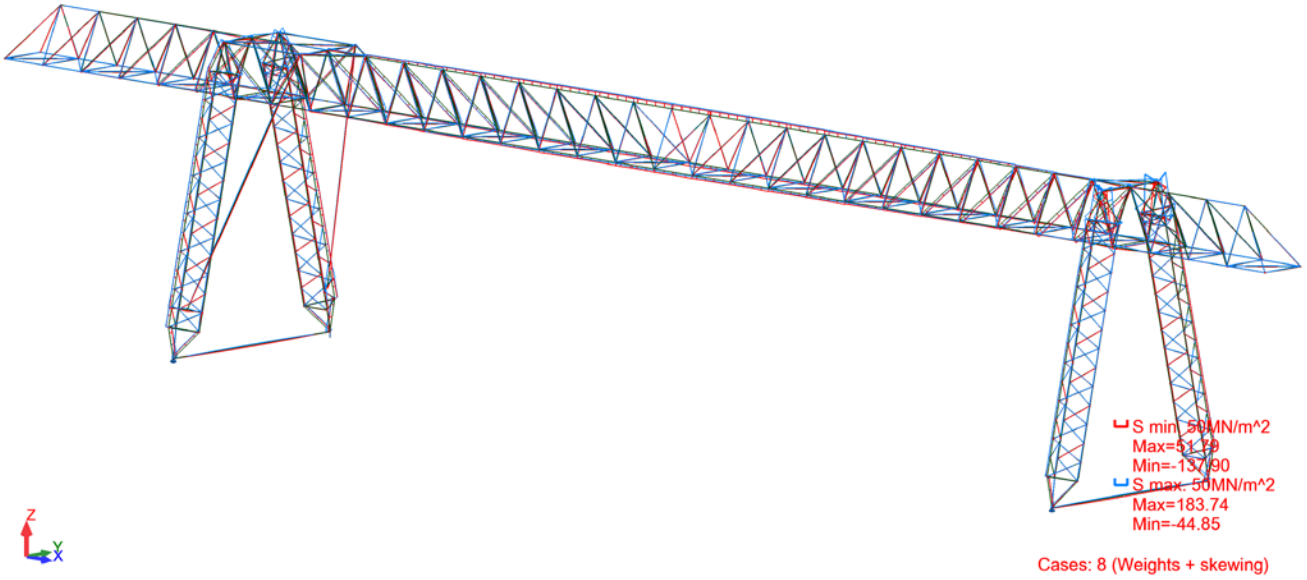

Figure 15: Stress distribution for the case with the skewing force calculated using JUS standard

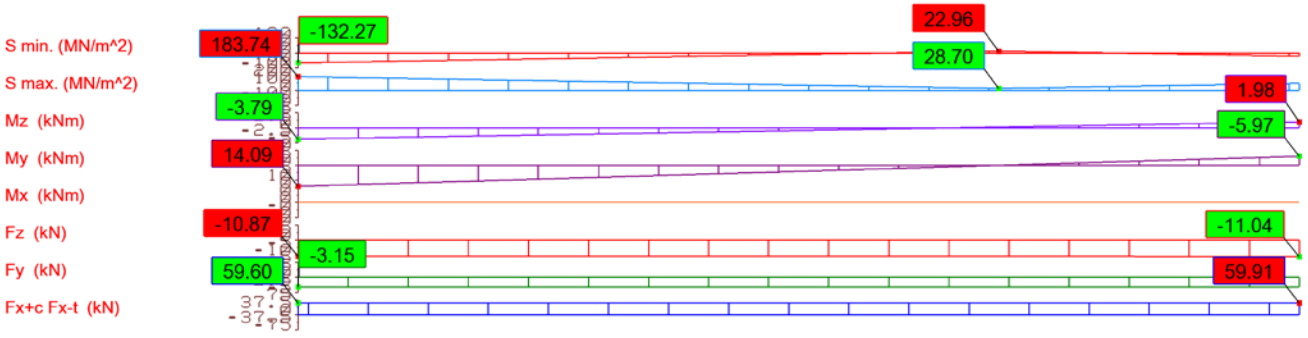

a) Eurocode 1

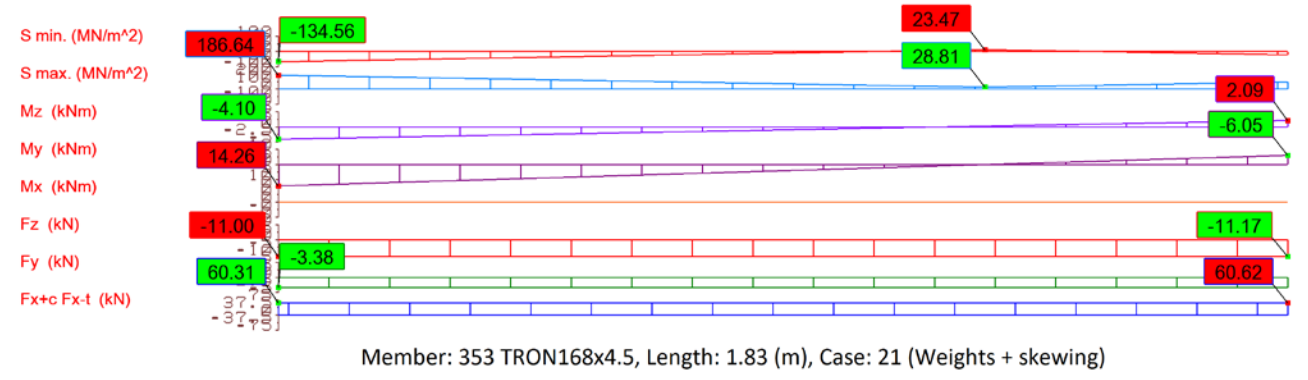

b) JUS

Figure 16: Stress distribution, moemntum, shear and axial diagrams for member 353

Table 8: The stress comparison for the critical member 353

Eurocode 1				*JUS*				*Δ (MPa)*			*δ [%]*		
	S max (MPa)	*S min (MPa)*	*Fx/Ax (MPa)*		*S max (MPa)*	*S min (MPa)*	*Fx/Ax (MPa)*	*S max*	*S min*	*Fx/Ax*	*S max*	*S min*	*Fx/Ax*
MAX	*183.74*	*45.31*	*51.97*	*MAX*	*186.64*	*45.34*	*51.98*	*-2.9*	*-0.03*	*-0.01*	*1.553793*	*0.066167*	*0.019238*
Member	*353*	*7*	*283*	*Member*	*353*	*7*	*283*						
Node	*212*	*6*	*159*	*Node*	*212*	*6*	*159*						
	S max (MPa)	*S min (MPa)*	*Fx/Ax (MPa)*		*S max (MPa)*	*S min (MPa)*	*Fx/Ax (MPa)*	*S max*	*S min*	*Fx/Ax*	*S max*	*S min*	*Fx/Ax*
MIN	*-39.1*	*-137.9*	*-46.55*	*MIN*	*-39.19*	*-140.27*	*-46.66*	*0.09*	*2.37*	*0.11*	*0.22965*	*1.689599*	*0.235748*
Member	*211*	*421*	*211*	*Member*	*211*	*354*	*211*						
Node	*112*	*259*	*112*	*Node*	*112*	*212*	*112*						

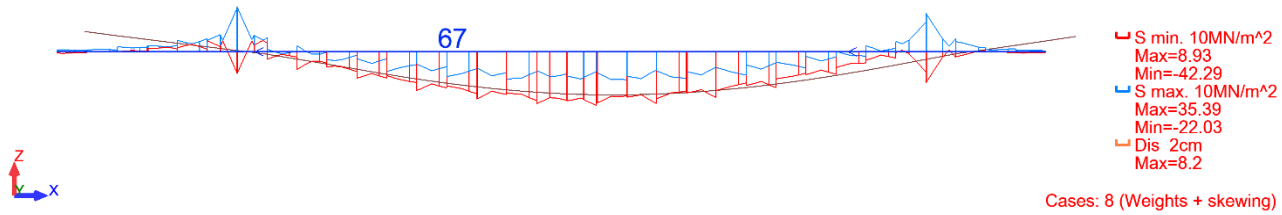

a) Eurocode 1

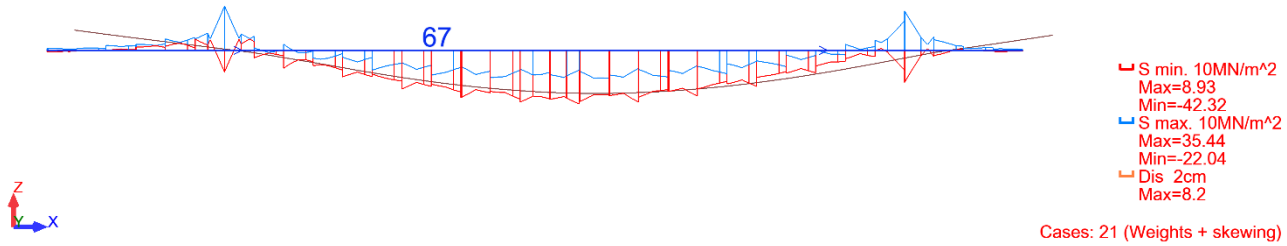

b) JUS standard

Figure 17: Stress distribution and deflection diagrams for the member 67

Table 9: Results comparison of the structural analysis for the member 67

Eurocode 1				*JUS*				*Δ*		*δ*	
	S max (MPa)	*S min (MPa)*	*Deformation (cm)*		*S max (MPa)*	*S min (MPa)*	*Deformation (cm)*	*S max (MPa)*	*S min (MPa)*	*S max (%)*	*S min (%)*
MAX	*35.39*	*8.93*	*8.2*	*MAX*	*35.44*	*8.93*	*8.2*	*0.05*	*0*	*0.14108*	*0*
Member	*67*	*67*	*67*	*Member*	*67*	*67*	*67*				
Point	*x = 0.182*	*x = 0.208*	*x = 0.541*	*Point*	*x = 0.1818*	*x = 0.2082*	*x = 0.5411*				
MIN	*-22.03*	*-42.29*	*0*	*MIN*	*-22.04*	*-42.32*	*0*	*-0.01*	*-0.03*	*0.0453*	*0.071*
Member	*67*	*67*	*67*	*Member*	*67*	*67*	*67*				
Point	*x = 0.576*	*x = 0.545*	*x = 0.532*	*Point*	*x = 0.5758*	*x = 0.5455*	*x = 0.5323*				

5. DISCUSSION AND CONCLUSIONS

The results of the analysis show that the skewing of the large span gantry crane plays an important part in the analysis of the structure. The figure 15 shows that the most critical part of the structure of the crane when skewing happens are the members that make up the elastic leg of the crane.

Even though the JUS and Eurocode 1 standards define skewing forces in different places within the

structure, diagrams shown in figures 16 and 17 show that the stress distribution is similar in both cases. The intensities of the skewing forces calculated in JUS and Eurocode 1, in case of this large span gantry crane differ by 7,01 % in favour of JUS standard. However, the maximum stress value in the structure, in the member 353 according to the table 8 is only 1,56 % higher when the skewing force was calculated using JUS standard, which implies that the forces in vertical plane have dominance over the skewing force.

The difference in the intensity of the skewing force did not show any change in the deflection of the main grinder, and for both cases, according to the table 9 and figure 17, it stayed unchanged.

ACKNOWLEDGEMENTS

This work has been supported by the Ministry of Science, Technological Development and Innovation of the Republic of Serbia, through the Contracts for the scientific research financing in 2023, 451-03-47/2023-01/200102 and 451-03-47/2023-01/200108.

REFERENCES

[1] F. Frendo, “Gantry crane derailment and collapse induced by wind load”, Engineering Failure Analysis, Vol. 66, pp. 479-488, (2016), doi: 10.1016/j.engfailanal.2016.05.008

[2] E. E. Vernon, M. E. Stevenson and J. L. McDougall, “Premature failure of steel gantry crane wheels”, Journal of Failure Analysis and Prevention, Vol. 4, pp. 16-18, (2004), doi: 10.1361/15477020420783

[3] J. Xiao, Y. Wu, X. Long and C. Xu, “Failure Analysis of Gantry Crane Slewing Bearing Based on Gear Position Accuracy Error”, Applied Sciences, Vol. 12(23), p. 11907, (2022), doi: 10.3390/app122311907

[4] M. Erosy, “A Proposal on Occupational Accident Risk Analysis: A Case Study of a Marble Factory”, Human and Ecological Risk Assessment: An International Journal, Vol. 21(8), pp. 2099-2125, (2015), doi: 10.1080/10807039.2015.1017878

[5] H. I. Jaafar, Z. Mohamed, J. J. Jamian, A. F. Z. Abidin, A. M. Kassim, and Z. A. Ghani, “Dynamic Behaviour of a Nonlinear Gantry Crane System”, Procedia Technology, Vol. 11, pp. 419–425, (2013), doi: 10.1016/j.protcy.2013.12.211

[6] N. Đ. Zrnić, V. M. Gašić, and S. M. Bošnjak, “Dynamic responses of a gantry crane system due to a moving body considered as moving oscillator”, Archiv.Civ.Mech.Eng, Vol. 15(1), pp. 243–250, (2015), doi: 10.1016/j.acme.2014.02.002

[7] I. Gerdemeli and S. Kurt, “Design and Finite Element Analysis of Gantry Crane”, Key Engineering Materials, Vol. 572, pp. 517–520, (2014), doi: 10.4028/www.scientific.net/KEM.572.517

[8] ASME B30.2-2005: Overhead and Gantry Cranes

[9] Eurocode 1. Actions on structures. Actions induced by cranes and machines. London: British Standards Institution, 2006.

[10] “Rules for the design of cranes”, British Standards Institution

[11] L. Sowa, Z. Saternus and M. Kubiak, “Numerical Modelling of Mechanical Phenomena in the Gantry Crane Beam”, Procedia Engineering, Vol. 177, pp. 225-232, (2017), doi: 10.1016/j.proeng.2017.02.193

[12] L. Sowa, T. Skrzypczak and P. Kwiatoń, “The effect of the gantry crane beam cross section on the level of generated stresses”, MATEC Web Conf., Machine Modelling and Simulations 2017 (MMS 2017), Vol. 157, (2018), doi: 10.1051/matecconf/201815702047

[13] T. Haniszewski, “Strength analysis of overhead traveling crane with use of finite element method”, Transport Problems, Vol. 9(1), pp. 19–26, (2014)

[14] D. Ostrić, “Dizalice”, Mašinski fakultet Beograd, (1992), ISBN 86 – 7083 – 199 – 6